Physica A 492 (2018) 1153–1167

Contents lists available at ScienceDirect

Physica A

journal homepage: www.elsevier.com/locate/physa

Modeling detour behavior of pedestrian dynamics under different conditions

Yunchao Qu [a], Yao Xiao [b], Jianjun Wu [a,b,*], Tao Tang [a], Ziyou Gao [a,b]

[a] State Key Lab of Rail Traffic Control & Safety, Beijing Jiaotong University, Beijing, 100044, China
[b] School of Transport and Transportation, Beijing Jiaotong University, Beijing, 100044, China

HIGHLIGHTS

- A modified social force model is proposed to describe the characteristics of the detour behavior.
- Voronoi diagram is included to define the alternative moving directions and describe the detour behavior.
- Three categories of factors and heuristic rules are proposed to describe detour behavior.
- The frequency of collision and average velocities under different situations were simulated and analyzed.

ARTICLE INFO

Article history:
Received 29 July 2017
Received in revised form 9 November 2017
Available online 2 December 2017

Keywords:
Pedestrian dynamics
Social force model
Detour behavior
Voronoi diagram

ABSTRACT

Pedestrian simulation approach has been widely used to reveal the human behavior and evaluate the performance of crowd evacuation. In the existing pedestrian simulation models, the social force model is capable of predicting many collective phenomena. Detour behavior occurs in many cases, and the important behavior is a dominate factor of the crowd evacuation efficiency. However, limited attention has been attracted for analyzing and modeling the characteristics of detour behavior. In this paper, a modified social force model integrated by Voronoi diagram is proposed to calculate the detour direction and preferred velocity. Besides, with the consideration of locations and velocities of neighbor pedestrians, a Logit-based choice model is built to describe the detour direction choice. The proposed model is applied to analyze pedestrian dynamics in a corridor scenario with either unidirectional or bidirectional flow, and a building scenario in real-world. Simulation results show that the modified social force model including detour behavior could reduce the frequency of collision and deadlock, increase the average speed of the crowd, and predict more practical crowd dynamics with detour behavior. This model can also be potentially applied to understand the pedestrian dynamics and design emergent management strategies for crowd evacuations.

1. Introduction

With the increase of activity frequency in big cities, crowd evacuation becomes an important problem in large public spaces. Increasing attentions have been devoted to the research of pedestrian dynamics to investigate the pedestrian evacuation behaviors [1,2], make managements and emergent plans of crowd evacuation [3], and improve the building inner structural design [4,5]. To quantitatively and qualitatively investigate the pedestrian dynamics, simulation method

* Corresponding author at: State Key Lab of Rail Traffic Control & Safety, Beijing Jiaotong University, Beijing, 100044, China.
E-mail address: jjwu1@bjtu.edu.cn (J. Wu).

https://doi.org/10.1016/j.physa.2017.11.044
0378-4371/

becomes a powerful tool with some advantages [6]. For examples, the development of computational power could afford us the ability to investigate the crowd behaviors in large-scale places, and large labor costs and potential safety problems especially in emergency situations could be avoided using simulation methods.

In decades, researchers have developed many microscopic and macroscopic pedestrian flow models that enable us to accurately describe the pedestrian movements and pedestrian behaviors [7], such as cellular automata model (CA), social force model (SFM), lattice gas model [8], agent based model [9], and heuristics based model [10]. Cellular automata model is a spatial-discrete model, and it divides the space into a series of uniform cells. Generally speaking, each pedestrian occupies a single cell, and it can move to one of its neighbor cells according to the transition probability at each time stamp. A popular approach to calculate the probability is to define a static and dynamic floor field for each cell, which is called floor field model (FF) [11–17]. This category of models have been successfully applied to study the crowd evacuation process in both of the uni-directional and bi-directional flows in different kinds of buildings, such as primary schools and urban transit stations [18–23].

In contrast, social force model is a spatial-continuous model, and it has been widely used in quantitatively simulating microscopic pedestrian dynamics due to its simple formulations and easy-extensible framework [24–26]. Based on the framework of the original social force model, many modifications have been developed to produce a more realistic behavior by introducing some intelligent rules, such as isolated pedestrian [27], leadership effect [28,29], waiting pedestrians [30], staircase [31], earthquake situation [32]. Under the framework of the force-based model, the concept of the centrifugal force is proposed to replace the repulsive force and considered the factors of the headway and the relative velocity between pedestrians [33,34]. Because this model can reproduce smoother trajectory than cellular automata model, and the dynamic properties and interactions between pedestrians can be better quantitatively described. This paper concerns on the spatial-continuous social force model and extends it to describe the detour behavior.

During the pedestrian movement, the detour behavior may occur in many cases, and the important behavior is a dominate factor of the crowd evacuation efficiency. Generally speaking, a crowd is always made up of heterogeneous pedestrians with different psychological and physiological attributes, and they always perform different behavioral and kinematic characteristics. For example, some pedestrians may walk fast and impertinently to pass over others, and some pedestrians may walk conservatively and cooperate with others. Especially, some pedestrians may walk in a relatively slow speed due to some special reasons, e.g., watching mobile phone, bending over to pick things up, etc. These people may block others and form a local congestion. The blocked pedestrians will detour the slower pedestrian to avoid potential collisions with them.

In the traditional social force models, the self-driven force is simply set to the direction that directly points to the destination [24], and the constant direction of self-driven force many lead to some more unreasonable phenomena due to lack of detour mechanism, e.g., oscillation and deadlock. Inspired by this factor, some modifications on social force model regarding the intelligent overtaking behavior have been presented to guide pedestrians to avoid collisions [35–38].

In addition, some heuristics strategies have been integrated into pedestrian modeling to deal with complex situations and predict smoother trajectories, e.g., vision heuristics-based rules [10], spatial–temporal separation behavior [39,40], velocity obstacle rules in motion planning [41,42]. Recently, the concept of Voronoi diagram has also been included to determine local density [43], analyze the characteristics of bottleneck motion [44], and density-based optimal velocity [45]. The alternative desired velocity directions are identified into three categories of elemental directions, and a heuristic method is used to calculate the final desired direction. Although detour behavior is closely related to the geometrical property of Voronoi diagram, the detour behavior is still less mentioned in the existing works.

To better explain the detour behavior, this paper integrates Voronoi diagram into the social force model with the modeling framework of Ref. [45]. Three factors including distance to Voronoi node, deviation angle, velocity difference are introduced to further model the detour behavior, and a Logit-based discrete choice model is then used to determine the final desired velocity direction. The impact of detour behavior on the frequency of collisions and the average speed will be analyzed by simulations, and the influence parameters analysis of bidirectional pedestrian flows will be also discussed.

The remainder of this paper is organized as follows. Section 2 describes the modeling framework and the social force model for pedestrian simulation. Section 3 introduces the concept of Voronoi diagram and its applications on detour behavior modeling. Section 4 designs a series of simulations to analyze the pedestrian detour behavior under different situations, and then a crowd video captured from a teaching building is applied to validate the proposed modified social force model. Section 5 gives a further discussion of this model and explores the future works.

2. Modeling framework

2.1. Social force model

In general, pedestrian behavior can be characterized into three categories [46]: the strategical level, the tactical level, and the operational level. In pedestrian movement, a pedestrian always firstly chooses a destination (e.g., an exit in a building), then decides an optimal intermediate desired direction and velocity, and finally adjusts his/her velocity to reach the temporary destination. The result of the model at the strategical level is a travel mode and a destination choice which will be the input of the tactical level. The route choice in the tactical level is a microscopic path from origin to destination including all crucial intermediate nodes. The model in the operational level is to explain the real-time trajectory and instantaneous response to surrounding information at each time stamp. This paper is concerned with the analyzing and modeling the characteristics of detour behavior at the operational level.

To better understand the mechanism of the social force model, a brief introduction of the model is given as follow. As done in most of space-continuous microscopic pedestrian models, social force model regards each pedestrian as a circle, and the motion of each particle is influenced by three kind of forces, which are self-driven force $\mathbf{f}_i^{drv}$ remote repulsive forces $\mathbf{f}_{ij}^{nc}$ and body contact forces $\mathbf{f}_{ij}^{c}$ with other pedestrians and obstacles. Here, i and j represent pedestrian. The total force $\mathbf{f}_i$ exerted on pedestrian i would be obtained by simply summing up all the forces by Eq. (1), and the acceleration will be calculated by the Newton's Second Law.

$$\mathbf{f}_i = \mathbf{f}_i^{drv} + \sum_j \mathbf{f}_{ij}^{nc} + \sum_j \mathbf{f}_{ij}^{c} \tag{1}$$

In these forces, self-driven force presents the personal intention of moving towards to destination, which can be calculated by Eq. (2).

$$\mathbf{f}_i^{drv} = \frac{1}{\tau}\left(v^{pre} \cdot \mathbf{e}^{pre} - \mathbf{v}_i\right) \tag{2}$$

where, τ is the relaxation time, v^{pre} is the magnitude of the desired velocity, $\mathbf{e}^{pre}$ is the desired velocity direction, and $\mathbf{v}_i$ is the current velocity.

Social force or remote repulsive force represents the individual intention of keeping a certain distance from others during walking. When other pedestrians are getting closer, he/she may feel uncomfortable or squeezed because its walking space is getting smaller and occupied by others. Hence, the repulsive force generated in the social force model is modeled as Eq. (3),

$$\mathbf{f}_{ij}^{nc} = k_{ij} \cdot \alpha \cdot \exp\left(\frac{r_{ij} - d_{ij}}{\beta}\right) \cdot \mathbf{e}_{ij} \tag{3}$$

$\mathbf{e}_{ij}$ is the unit vector pointing from pedestrian i to pedestrian j. r_i is the radius of pedestrian i, and r_{ij} is the sum of their radii $r_{ij} = r_i + r_j$. d_{ij} is the distance between the two pedestrians. α, β are parameters. The pedestrian only reacts to obstacles and pedestrians in their vision fields. The perception field is supposed to be a 180° vision field, and other pedestrians who are not in the field are not taken into consideration. Here, the coefficient k_{ij} is introduced as Eq. (4), and $\mathbf{e}_i$ is the united vector of the walking direction of pedestrian i.

$$k_{ij} = \begin{cases} \mathbf{e}_i \cdot \mathbf{e}_{ij}, & \mathbf{e}_i \cdot \mathbf{e}_{ij} > 0 \\ 0, & \text{otherwise} \end{cases} \tag{4}$$

Contact force or physical force is similar with the repulsive force, which represents the repulsive force when pedestrians get close to each other. It could be divided into two categories, the first one is to counteract the body compression and called "body force" $\mathbf{f}_{ij}^{c_1}$, while the second one is to impede relative tangential motion and called "sliding friction force" $\mathbf{f}_{ij}^{c_2}$. Herein, the physical force is given as Eq. (5),

$$\mathbf{f}_{ij}^{c} = \mathbf{f}_{ij}^{c_1} + \mathbf{f}_{ij}^{c_2} = \gamma_1 \cdot g\left(r_{ij} - d_{ij}\right) \cdot \mathbf{e}_{ij} + \gamma_2 \cdot g\left(r_{ij} - d_{ij}\right) \cdot (\mathbf{v}_j - \mathbf{v}_i) \cdot \mathbf{t}_{ij} \tag{5}$$

Here, γ_1 and γ_2 are constant parameters, $\mathbf{t}_{ij}$ is the tangential direction, and $g\left(r_{ij} - d_{ij}\right)$ is used to indicate the contact status of pedestrian i and pedestrian j. If the distance d_{ij} between two pedestrians i and j is smaller than the sum of their radii $d_{ij} < r_i + r_j$, the two pedestrians will be regarded as contacting or colliding with each other. The physical force is generated only if the pedestrian are contacted, which is shown as Eq. (6).

$$g\left(r_{ij} - d_{ij}\right) = \begin{cases} r_i + r_j - d_{ij}, & r_i + r_j - d_{ij} \geq 0 \\ 0, & \text{otherwise} \end{cases} \tag{6}$$

More details and the parameters refer to Ref. [25].

2.2. Detour behavior

Detour behavior is one of the most important behaviors during walking, and this kind of behavior always occurs when pedestrians are facing the following conditions: (1) static obstacles or standing pedestrians, (2) moving obstacles/pedestrians with same directions, (3) moving obstacles/pedestrians with opposite directions. For example, during rush hours, some hurry passengers might walk or even run at a higher speed, detour other pedestrians, and rush through the crowd in the platform to catch a train. In bidirectional pedestrian flows, pedestrians always make detours in advance to avoid pedestrians from the opposite direction. The aims of the detour behavior are to achieve a higher speed and to avoid potential collisions with others.

The original social force model is capable of reproducing many self-organized phenomena in real world, such as arching queue, dynamic lane formation, stripe formation and bottleneck oscillations [26]. However, if the detour behavior is ignored, the original social force model will produce some unrealistic collisions between pedestrians, heavy congestion, and even deadlock phenomenon in a low density condition.

Fig. 1 illustrates an unrealistic scenario that two pedestrians i and j are walking towards each other. In the traditional social force model, the desired direction of the self-driven force is simply set to the direction to the destination, and it is

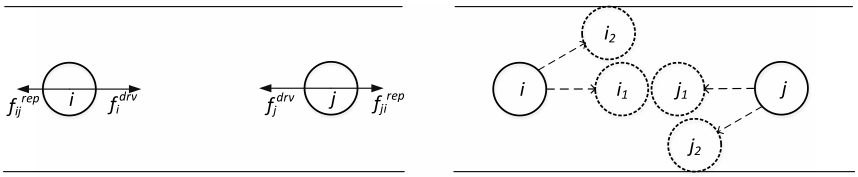

Fig. 1. Pedestrians toward each other in the traditional social force model.

not dynamically updated. Two pedestrians are located at the left center and right center of the corridor, respectively. The destination of pedestrian i is the right end of corridor, and the destination of pedestrian j is the left end of corridor. If simply setting the desired directions (1, 0) and (−1, 0) for pedestrians i and j, the pedestrians will walk in the opposite walking directions, and the resultant force of the self-driven force and the interaction forces will finally cause a collision between them and even lead to the occurrence of a unreasonable deadlock situation, e.g., the final positions i_1 and j_1. However, in reality, the two pedestrians might change the walking directions and make a detour during the walking process, e.g., the final positions i_2 and j_2.

To improve the simulation performances of the original social force model, pedestrian's individual detour behavioral characteristics and topological interactions with neighbors should be integrated to describe the desired direction and the self-driven force. Moussaid et al. [10] regarded pedestrians as intelligent agents and proposed some heuristic rules. In that model, the social force was integrated into the self-driven force, and an optimization model was used to select the desired velocity. Inspired by the modeling framework. Xiao et al. [45] introduced the concept of Voronoi diagram to model pedestrian dynamics. In that work, pedestrians were assumed to be homogeneous and rational, and each pedestrian could optimally select its desired velocity direction from three categories of directions, which were detour direction, destination direction, and fine-tuning direction. However, in reality, pedestrians are always with different behavior modes, and a crowd may be made up of heterogeneous pedestrians. Besides, detour behavior is more complicated than that was described in the existing references.

This paper focuses on modeling detour behavior in the operation level and modifying the self-driven force in Eq. (1) from two aspects: (i) preferred detour direction $\mathbf{e}^{pre}$: deciding which person and which side to make a detour; (ii) preferred detour velocity v_0: deciding how fast to detour a pedestrian. The following section will detailed discuss the properties of detour behavior and propose a comprehensive detour model.

3. Detour model

3.1. Voronoi diagram

Inspired by Refs. [43–45], the concept of Voronoi diagram is applied to model the detour behavior. We firstly introduce the Voronoi diagram and its applications to pedestrian dynamics modeling. Given a set of points $N = \{(x_1, y_1), (x_2, y_2), \ldots, (x_n, y_n)\}$ in a two-dimensional space, a Voronoi diagram splits the space into n convex polygons. Each point in the specific set is located in a single polygonal region, which is defined as Thiessen polygon or Voronoi cell (VC). An edge of a Voronoi cell, namely Voronoi link (VL), is located on the mid-perpendicular of the neighboring points, and shared by two adjacent Voronoi cells. A vertex of a Voronoi cell is defined as a Voronoi node, and it is the cross point of two or more Voronoi links. A Voronoi link is the mid-perpendicular of adjacent pedestrians, while the Voronoi node (VN) is the intersection of the Voronoi links. Regarding the pedestrians as specific points, a Voronoi diagram of pedestrians could be efficiently calculated by existing algorithms with complexity of O($n$lg$n$) [47]. Fig. 2 illustrates an example of Voronoi diagram including 100 pedestrians.

Because a Voronoi node is the cross point of two adjacent Voronoi links, the direction to the Voronoi node could avoid an excessive approach to any of the two pedestrians. According to the features of Voronoi diagram, a Voronoi cell contains all points closer to the related pedestrian than to others, and therefore, the space of Voronoi cell can be regarded as the personal region of its occupied pedestrian. In the Voronoi cell of a pedestrian, the moveable distance in its personal region can be defined as the distance from the position of the pedestrian to the boundary of the Voronoi cell. Pedestrians can walk a longer moveable distance along the direction to Voronoi node than other directions. Therefore, the direction pointing to a Voronoi node can be regarded as a most likely overtaking, bypass or detour direction. Assume that the position of pedestrian i is X_i and the position of Voronoi node k is N_k, the detour behavior could be clearly identified as Eq. (7).

$$\mathbf{e}^{detour} = \frac{N_k - X_i}{\|N_k - X_i\|} \tag{7}$$

With non-degeneracy assumption, each Voronoi node has exactly three Voronoi edges, which means that each Voronoi node has three nearest neighbor pedestrians. The detour direction can be regarded as walking through its two neighbor pedestrians. In addition, restricted by the factor of vision, people usually interact with their neighbors within their vision

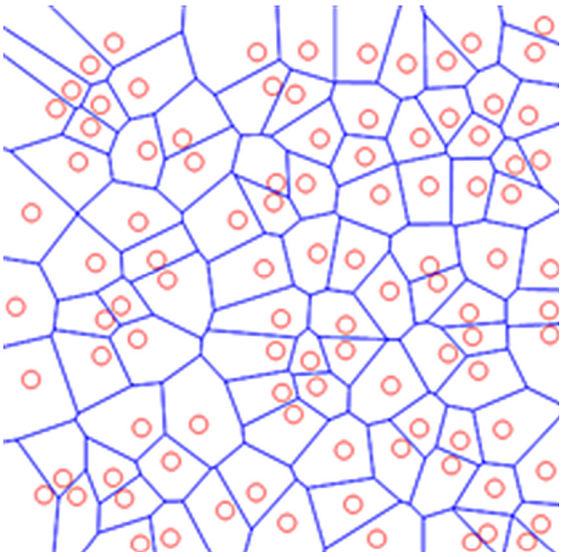

Fig. 2. Voronoi diagram of pedestrians. Each circle represents a pedestrian, and each line represents a Voronoi link.

fields ϕ. To determine the alternative Voronoi nodes in one's vision field, the included angle between the velocity and the direction of pointing to Voronoi node k is computed by Eq. (8).

$$\theta_k = \left\langle \overrightarrow{X_i N_k}, \overrightarrow{V_i} \right\rangle \tag{8}$$

If the angle is smaller than ϕ (i.e., $\phi = 75^\circ$), node k is identified as an alternative node in the vision field. As shown in Fig. 3, the directions pointing to all Voronoi nodes $\mathbf{d}_1$, $\mathbf{d}_2$, $\mathbf{d}_3$, $\mathbf{d}_4$, $\mathbf{d}_5$ are illustrated, and the directions $\mathbf{d}_3$, $\mathbf{d}_4$ are alternative detour directions in the vision field. The next two questions are to decide the direction of the preferred detour velocity among the alternative detour directions and to determine the magnitude of the detour velocity.

3.2. Detour velocity decision

In the traditional social force model, the interactions with other pedestrians and obstacles lead to the changing of walking direction. Inspired by the geometrical characteristics of Voronoi diagram, an alternative detour direction has been introduced in Section 3.1. A detour direction points from the current position to one of the Voronoi nodes of its occupied Voronoi cell. To determine a most possible desired detour direction, three factors will be taken into consideration, which are the distance to each Voronoi node, the angle between the detour direction and the velocity, and the velocity difference with neighbor pedestrian. Correspondingly, three heuristic rules are proposed to model the detour direction choice behavior.

The first factor is the distance to Voronoi node l_k, and the heuristic rule is that people are willing to choose a larger distance to Voronoi node to move fast. The distance between the current location and each Voronoi node represents the potential moveable distance to each adjacent cell. If the distance is large, the pedestrian is able to achieve a higher speed along the direction; otherwise, the pedestrian needs to slow down to avoid potential collision with others.

The second factor is the deviation angle θ, and the second heuristic rule is that people prefer to choose a detour direction with small deviation angle with the current velocity. If the detour direction deviates from the velocity a large angle, the pedestrian will struggle to change its current velocity to the preferred velocity.

The third factor is the velocity difference with other pedestrian $\Delta v_k = \sum_{p \in VN_k} \left\| \mathbf{v}_i - \mathbf{v}_p \right\|$, and the heuristic rule is that pedestrians prefer to detour others with larger velocity differences. If the velocity difference Δv_k is larger, the pedestrian is more likely to be blocked by neighbor pedestrians, and the Voronoi node is the most possible detour direction.

Considering the above three types of influence factors and heuristic rules, the utility function U_k of choosing Voronoi node k as detour direction is detailed described as Eq. (9). To tradeoff all factors and make the utility function reasonable, the influence factors are dealt with dimensionless treatment, and a linear combination is proposed to integrate the factors. Here, three parameters $\lambda_1, \lambda_2, \lambda_3$ are weighed to each factor.

$$U_k = \lambda_1 \frac{l_k}{l_{\max}} + \lambda_2 \cos\theta_k + \lambda_3 \frac{\Delta v_k}{\sum_p \left\| \mathbf{v}_p \right\|}, \forall k \in N, (\lambda_1 + \lambda_2 + \lambda_3 = 1, \lambda_1, \lambda_2, \lambda_3 \geq 0) \tag{9}$$

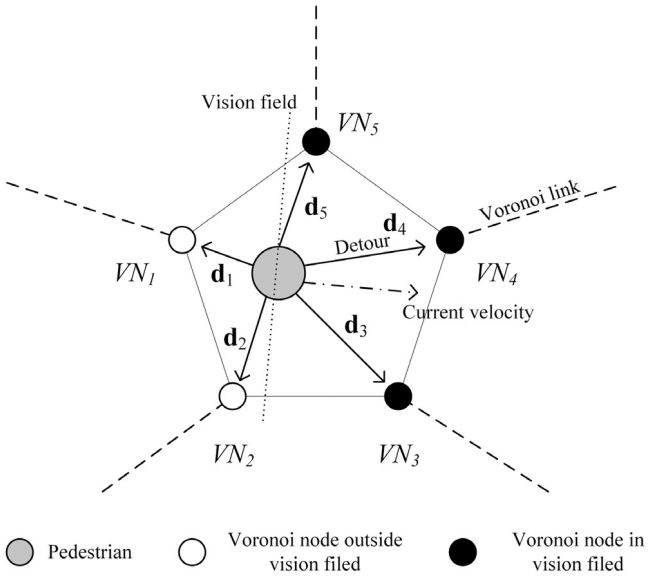

Fig. 3. Illustration of alternative detour directions.

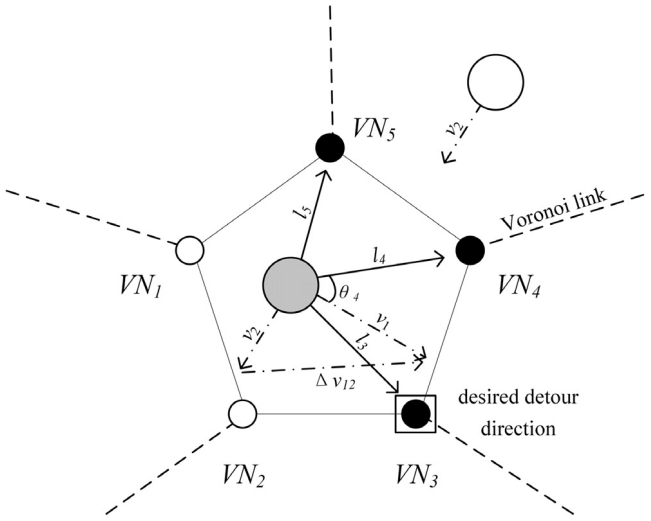

Fig. 4. Illustration of a desired detour direction choice.

After acquiring the utility of each direction, a logit-based model is to determine the probability of choosing each detour direction by Eq. (10). Fig. 4 illustrates an example of choosing a desired detour direction.

$$p_k = \frac{\exp(U_k)}{\sum_{j\in N} \exp(U_j)} \tag{10}$$

In some situations, several pedestrians may choose the same Voronoi node as their temporary destination. These pedestrians would head for the same location and cause conflicts and even serious collisions. However, in reality, pedestrians are able to avoid some potential conflicts, so extra rules should be included to improve the performance. To solve some potential conflicts, a radical probability pr is formulated in Eq. (11), which represents the probability of pedestrian i choosing the preferred detour direction.

$$pr_i = \frac{\exp(p_i)}{\sum_{j\in N} \exp(p_j)} \tag{11}$$

The radical probability are compared among the related pedestrians. The most radical pedestrian would remain the original detour direction, while the other pedestrians will change their desired detour directions to other Voronoi nodes. The sub-optimal Voronoi nodes are considered until there are no feasible detour direction.

It should be mentioned that pedestrians will not make a detour all the time, and it needs to decide whether a pedestrian needs to make a detour or not. Considering the distance to the front pedestrian j and the relative velocity, a pedestrian will make a detour when $d_{ij} - \tau \cdot \left(\mathbf{v}_i - \mathbf{v}_j\right) \mathbf{e}_{ij} < 0$; otherwise, the pedestrian will keep its original destination direction. In conclusion, the modified direction of the self-driven force is given as,

$$\mathbf{e}^{dir} = \begin{cases} \mathbf{e}^{detour}, & d_{ij} - \tau \cdot \left(\mathbf{v}_i - \mathbf{v}_j\right) \mathbf{e}_{ij} < 0 \\ \mathbf{e}^{des}, & \text{otherwise} \end{cases} \tag{12}$$

where $\mathbf{e}^{detour}$ is the unit vector of the detour direction to the selected Voronoi node k, $\mathbf{e}^{des}$ is the unit vector pointing to the destination.

The remaining question is to determine the magnitude of the desired velocity. A time period τ is required for the pedestrian to stop in the case of an unexpected obstacle, pedestrians should compensate for this delay by keeping a safe distance [10]. Here, the safe distance l_k is the distance to the selected Voronoi node k. As a result, a pedestrian prefers to maintain a distance from the current location to the selected Voronoi node within a relaxation time τ. Assuming that the velocity cannot exceed the maximum velocity $v_{\max}$, the desired velocity can be calculated by Eq. (13).

$$v^{pre} = \min\left(v_{\max}, \frac{l_k}{\tau}\right) \tag{13}$$

3.3. Simulation procedure

In the previous sections, the modified self-driven force and body contact force are formulated. According to Newton' second law, the update rules of pedestrians' movement with detour behavior can be given as follows.

(1) Load scenario, initialize the positions of pedestrians, and set parameters in this model. Set simulation time $T = 0$, and the total simulation time T_{total}.
(2) Calculate the Voronoi diagram of pedestrians according to the current locations of pedestrians, and generate Voronoi nodes for each cell.
(3) For each pedestrian i,
   (a) Calculate the potential detour direction, and decide whether to make a detour by the vision files. If the pedestrian plans to make a detour, determine an optimal detour direction for him/her by Eqs. (7)–(10);
   (b) Solving the potential conflicts by Eq. (11), and the desired direction by Eq. (12);
   (c) Calculate the magnitude of desired velocity by Eq. (13), and contact force by Eq. (5).
   (d) Calculate the acceleration $\mathbf{a}_i(t) = \mathbf{f}_i(t)/M$;
(4) Update all pedestrians' locations $\mathbf{x}_i(t)$ and velocities $\mathbf{v}_i(t)$.

$$\mathbf{x}_i(t + \Delta t) = \mathbf{x}_i(t) + \mathbf{v}_i(t) \cdot \Delta t + \mathbf{a}_i(t) \cdot (\Delta t)^2, \mathbf{v}_i(t + \Delta t) = \mathbf{v}_i(t) + \mathbf{a}_i(t) \cdot \Delta t \tag{14}$$

(5) Terminate. If the system satisfied the terminal criterion $T = T_{total}$ or all pedestrians evacuated, stop. Otherwise, set $T = T + 1$ and go to step (2) to continue the simulation.

4. Simulation and validation

In this section, numerical experiments were implemented to simulate pedestrian dynamics under different conditions to investigate the properties of the proposed models. The simulation scenarios included unidirectional pedestrian flow, bidirectional pedestrian flow and crowd walking with static and moving obstacles. All the experiments were implemented on a 10 m × 3 m straight corridor scenario, which was detailed described in the following sub-sections. Without special explanations, the initial position of pedestrian is randomly generated in simulation.

In Section 4.1, a few of pedestrians were initialized in the corridor, and the trajectories of all pedestrians were extracted to show that our model was able to solve the potential conflicts between pedestrians. Besides, a unidirectional pedestrian flow walking through several static obstacles was simulated to illustrate the characteristics of aggregated trajectories. In Section 4.2, a more complicated bidirectional pedestrian flow was implemented to analyze the impact of detour behavior on evacuation efficiency. A segment of crowd video captured in real world was used to validate our model. The influences of different parameters on the simulation results were also studied in Section 4.2.2. Without special introductions, the parameters of the original social force model and our model were listed in Table 1.

Table 1
Parameters setting in social force model and our model.

Parameter	Model	Value	Definition
τ	Both	0.5 s	Relaxation time in Eqs. (2) and (3)
α	SF	2000 N	For social force calculation in Eq. (3)
β	SF	0.8 m	For social force calculation in Eq. (3)
γ_1	Both	120 000 N/m	For contact force calculation in Eq. (5)
γ_2	Both	240 000 N/m^2	For contact force calculation in Eq. (5)
$\lambda_1, \lambda_2, \lambda_3$	Our model	To be determined	Utility function in Eq. (9)
v_{max}	Both	5 m/s	Maximal velocity
M	Both	60–80 kg	Weight of pedestrian
r	Both	0.15–0.25 m	Radius of pedestrian
Δt	Both	0.01 s	Simulation time interval in Eq. (14)

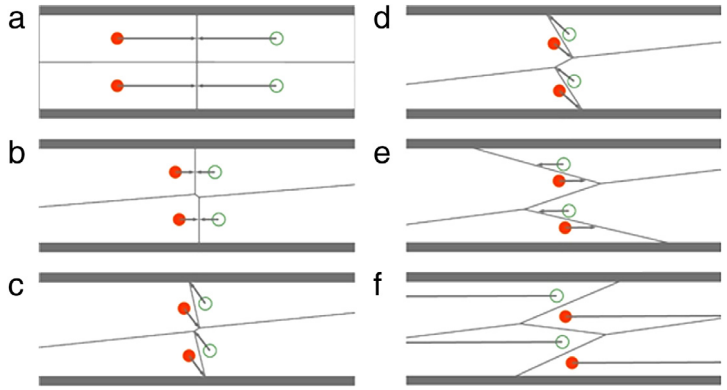

Fig. 5. Examples of pedestrian detour behavior in modified social force model.

4.1. Simulation

4.1.1. Pedestrians moving towards

Four pedestrians are uniformly and symmetrically distributed in the corridor, and the coordinates of them are (1, 0.75), (1, 2.25), (9, 0.75), (9, 2.25), respectively (Fig. 5a). Two pedestrians marked by solid circles move from left to right, and the other two pedestrians marked by hollow circles move from right to left. The Voronoi links are illustrated by the lines, and the arrow lines represent the directions of the self-driven forces of all pedestrians.

At the beginning stage, the pedestrians are walking in the desired directions to their destinations. They are in the opposite directions, and they are getting closer to each other (Fig. 5b). For a pedestrian, the distance between the current location and the Voronoi link becomes smaller until he/she reaches the boundary of the Voronoi cell. As a result, the pedestrian searches for a possible detour direction and finally selects an optimal Voronoi node as the moving target of self-driven force (Fig. 5c). Influenced by the self-driven force, pedestrians start to make a detour to avoid the potential collisions (Fig. 5d). During the detour phase, the Voronoi node is regarded as the temporary target of self-driven force. Once the front pedestrian is not blocked by the other pedestrians, the pedestrian will reselect the original destination as the direction of self-driven force (Fig. 5e). Inspired by the self-driven force pointing to the destination, the pedestrians finally reach the end of corridor (Fig. 5f).

In the traditional social force model, collisions might occur due to the opposite desired directions. Compared with the traditional model, the conflicts could be easily and quickly solved without any collision in our model. A more realistic detour trajectory is obtained by dynamically adjusting the desired direction of self-driven force.

4.1.2. Walking through static obstacles

In the experiments, a certain number of pedestrians were initialized in the corridor with the same walking direction, and all of them were set to move from left to right periodically (periodic boundary). If pedestrians left from the right edge of the corridor, they would immediately re-enter the corridor from the left edge. Five static obstacles were located in the corridor, and the coordinates of them were (3, 1.1), (3, 2.5), (5, 1.8), (7, 1.1), (7, 2.5), respectively. Both traditional social force model and our model were applied to simulate the unidirectional flow with static obstacles. The total number of pedestrians increased from 5 to 50.

To obtain more stable results, each simulation lasted 5000 time steps and repeated 10 times, and the number of collisions and average speed of the last 500 time steps were recorded. Fig. 6 illustrates the trajectories of pedestrians, and it is shown that the pedestrians tend to make detours when they get close to the obstacles. There are mainly two detour routes near

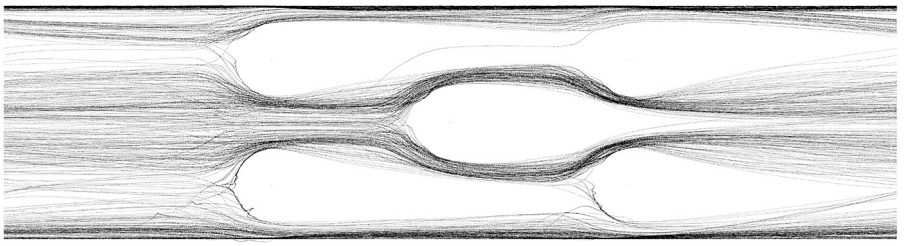

Fig. 6. Trajectory of unidirectional flow with five obstacles in corridor.

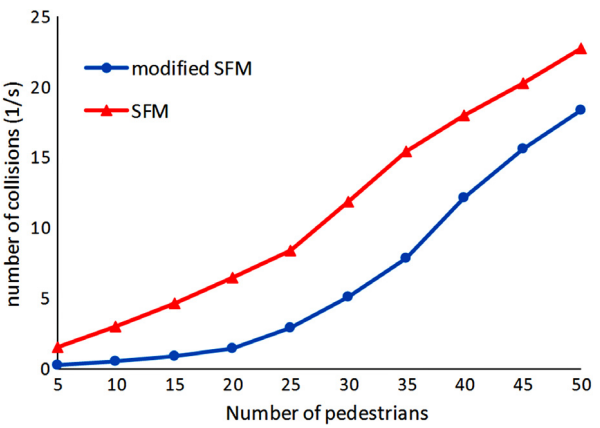

(a) Comparison of the collision times among SFM and modified SFM of unidirectional flow with five obstacles.

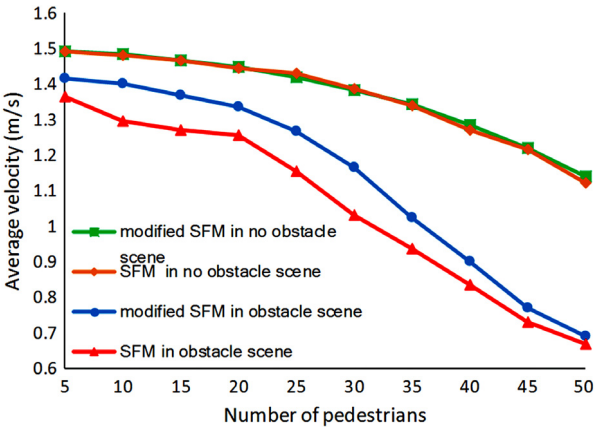

(b) Comparison of the average velocity among SFM in spacious scene, modified SFM in spacious scene, SFM in obstacle scene and modified SFM in obstacle scene.

Fig. 7. Simulation results of detouring obstacles.

each obstacle, and pedestrians prefer to walk in the center of the corridor than walk along the wall. By making detours, pedestrians are able to avoid collisions with the obstacles. In this simulation, the value of parameters are set to the value $\lambda_1 = 0.2, \lambda_2 = 0.5, \lambda_3 = 0.3$.

Due to the limitation of kinetic force-based simulation framework, the overlapping phenomenon between pedestrians cannot be absolutely avoided in the model with detour behavior, even if the pedestrians move in a very small time step $\Delta t \approx 0$ s. The number of collisions are recorded to compare our model with the original social force model. Besides, the average speed is calculated to evaluate the performance of the models.

Fig. 7(a) compares the number of collisions during the walk by the two models, and the modified social force model generates less collisions than the original model. To further investigate the performance of this model, we remove the obstacles and re-simulate the unidirectional pedestrian flow. Fig. 7(b) compares the average velocity of the crowd under two scenarios. The obstacles are the bottlenecks in the corridor, so pedestrians will reduce their walking velocities to detour obstacles, and the average velocity in the non-obstacle scene (e.g., 1.1 m/s, 50 pedestrians) is larger than obstacle scene (e.g., 0.7 m/s, 50 pedestrians). By comparing the average velocity, the modified social force model (e.g., 1.27 m/s, 25 pedestrians) can obtain a larger speed than the traditional model (e.g., 1.15 m/s, 25 pedestrians), and it is implied that the modified social force model could reduce the frequency of collisions.

4.2. Validation

4.2.1. Individual walking duration validation

In the section, the proposed model is applied to validate the individual walking process in a building. To test the performance of our model for in real world simulation, a video of pedestrians walking in the hall of a teaching building of Beijing Jiaotong University is recorded. There are nine entrances marked with "A" to "I", respectively. The camera is a trapezoid zone within red line boundaries. During the observation period, some students were crossing the hall from one of the entrance to another, and some other students were standing at the hall for a short while. The sketch map of the building is shown in Fig. 8. The video lasted for about 5 min, and we only selected a segment of 35 s as our research objectives. During the time period, there were 14 pedestrians (5 groups) standing still in the camera region. These pedestrians were regarded

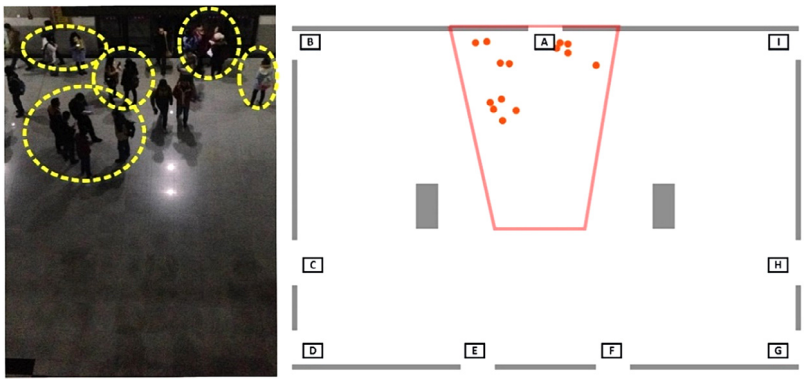

Fig. 8. Sketch map of the hall of the building and the camera region. The region is 45 m × 30 m, the width of Exit A, D, E, F, G is 3 m, the width of Exit B, I is 2.5 m, the width of Exit C, H is 4 m. The video region is a trapezoid, the lengths of the bases are 14 and 8 m, and the height is 14.8 m.

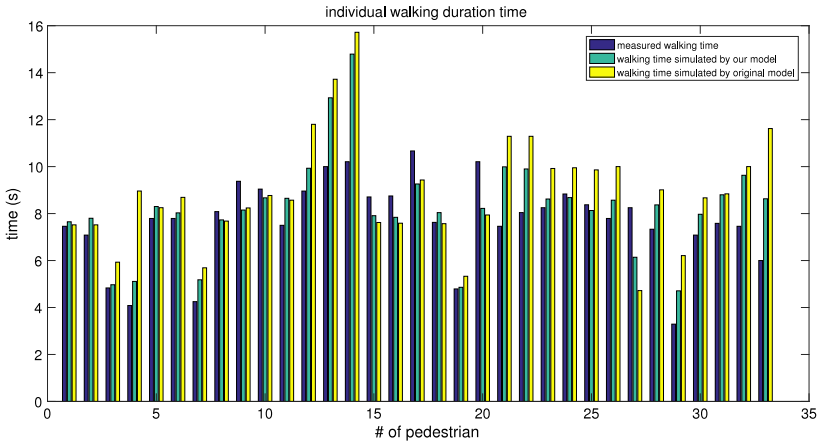

Fig. 9. Comparison of walking duration time simulated by different models.

as temporary obstacles for others. During the research period, there were 33 pedestrians entering into the camera region, bypassing the other pedestrians and leaving the camera region. The enter time, leave time and entrance number of each pedestrian were recorded. Although the size of the crowd was small, there were several pedestrians detouring others.

Both the original and modified social force model were used to simulate the moving process of pedestrian dynamics. 14 standing pedestrians were initially placed in the given locations, and 33 moving pedestrians entered into the camera region in the certain time with a determined destination exit. The simulation of each model repeated 10 times, and the walking duration time was compared in Fig. 9.

In the experiment, a pedestrian might frequently meet the standing pedestrians and other moving pedestrians to different destinations. Dealing with the conflicts with the standing and passing pedestrians would be the critical factor to determine the crossing time in the simulation. The crossing times and relative errors of these 33 pedestrians were adopt to evaluate the performance of the simulation models. Fig. 11 illustrates the comparison results of the two model. The relative errors of modified social force model are represented by the solid line, and the relative errors of the traditional social force model are represented by the dashed line. It is found that most of the relative errors calculated by the modified social force model are less than the traditional social force model, especially for pedestrians #4, #29, #33.

To make a further investigation, the specific movement process of pedestrian 4 (located in the red dashed circle) in both models are explored, and the snapshots of the simulations were shown in Fig. 10. Pedestrian 4 enters from the entrance A and regards the entrance B as the destination. The two models present different walking directions. Under the framework of traditional social force model, the resultant force would be difficult to guide the pedestrian avoid collisions, and hence lead to a delay of crossing time. Under the framework of modified social force model, the pedestrian could regard the Voronoi node as the object of self-driven force and avoid the potential collisions. The simulation result also indicated that the modified social force model could reduce the walking time by taking the detour behavior into account, and it agreed with the realistic pedestrian movements better than the original social force model.

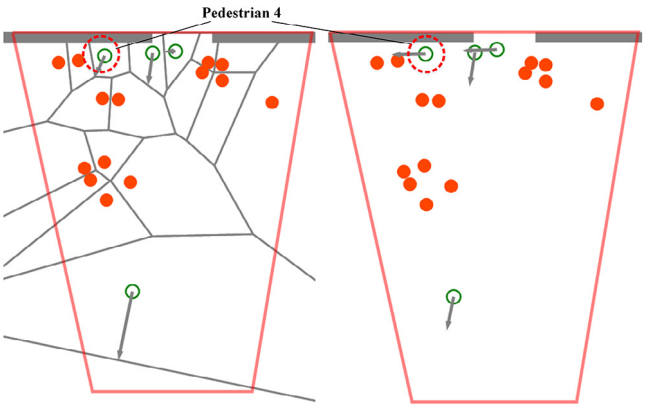

Fig. 10. Comparison of the direction of self-driven force in modified SFM and SFM. The orange circles represent the standing pedestrians, while the green circles represent the passing pedestrians. The gray arrows represent the direction of self-driven force of the passing pedestrians. (For interpretation of the references to color in this figure legend, the reader is referred to the web version of this article.)

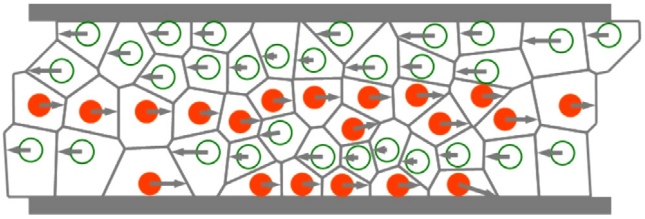

Fig. 11. A snapshot of bi-directional flow. 50 pedestrians walk in the 10 m × 3 m corridor. The orange solid circles represent the pedestrians head for the right side of the corridor and the green hollow circles represent the pedestrians head for the left side. 4 lanes are formulated in the corridor.

4.2.2. Bidirectional flow

Although many experimental and numerical studies have been performed for both unidirectional and bidirectional flow scenarios [21–23,48], little attention has been paid to analyze the characteristics of detour behavior. Compared with unidirectional pedestrian flow scenarios, potential conflicts occur more frequently in bidirectional flows, and detour behavior may affect the flow efficiency. To quantitatively understand the effect of detour behavior on dynamics characteristics in bidirectional flow, this section will discuss their relationships by the simulation approach.

A scenario of bidirectional pedestrian flow (Fig. 8) was simulated in the corridor. In the initial stage, pedestrians were randomly located in the corridor, and their speeds were all set to zero. The pedestrians were divided into two groups, the first group of pedestrians were represented by the orange solid circles head for the right end of the corridor, and the second group of pedestrians were represented by the green hollow circles head for the left end of the corridor. The numbers of the pedestrians in each group were same. The gray arrows represented the direction of self-driven force of each individual. Driven by the desired driven force, the pedestrians walked toward the ends of corridor. From the snapshot of Fig. 11, the lane formation phenomenon could be found.

In this simulation, the value of parameters of the linear combination parameters (λ_1, λ_2, λ_3) listed in Table 1 are set to different values to analyze their effects on crowd average speed. According to the constraint $\lambda_1 + \lambda_2 + \lambda_3 = 1$, the value of one parameter (e.g., λ_3) can be determined by the other two parameters (e.g., λ_1, λ_2). Here, we change the values of λ_1, λ_2 from 0.1 to 0.9 with the constraint $\lambda_1 + \lambda_2 < 1$. In simulation, 50 pedestrians walk towards in a corridor with 25 pedestrians in each direction, and the desired velocity for each pedestrian is 1.5 m/s. During the simulation, the average velocity $\overline{v}$ of the crowd is recorded by the following equation. Here, the total simulation time T is 5000 time intervals (50 s). The simulation results are shown in Fig. 12.

$$\overline{v} = \frac{\sum_{i,t} |v_{ix}(t)|}{T \cdot N} \tag{15}$$

According to the simulation results, the average speed of the crowd achieves at the maximum value 1.01 m/s. Assuming that λ_1 is given a fixed value, the average speed first decreases and then grows with the increasing of the value of λ_2. It implies that pedestrians will be mainly affected by the first and second factors, i.e., distances and deviation angles to the alternative Voronoi nodes. Besides, the average speed is at a high value when the parameters are set to $\lambda_1 + \lambda_2 = 0.9$. In the following analysis, the parameters will be set to $\lambda_1 = 0.7$, $\lambda_2 = 0.2$, $\lambda_3 = 0.1$.

We then analyze the total collision times using the same statistics method proposed in Section 4.1. Fig. 13(a) compares the number of collisions of the modified social force model and the traditional social force model. The modified social force

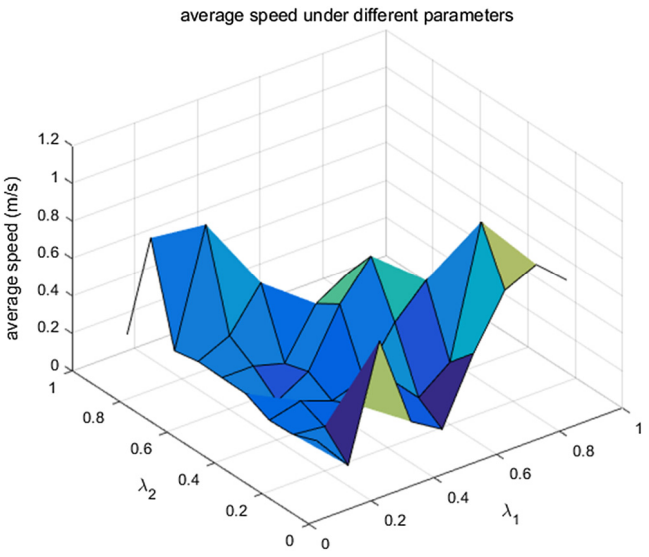

Fig. 12. Average flow under different parameter combinations.

model shows less collisions than the traditional social force model in the simulation. In the modified social force model, a pedestrian could adjust the direction of self-driven force to keep away from the oncoming pedestrians. Hence, a more practical walking behavior could realize and less collisions occur.

The average velocity of unidirectional and bidirectional flow in both models are collected as shown in Fig. 13(b). Under the situation of unidirectional flow, the simulated velocity–density relationships by the two models are nearly same. It is because that the detour behaviors occur less frequently, and the average velocity maintains at a large value with the growing of pedestrian numbers. In contrast, under the situation of bidirectional flow, the simulated results by the two model are quite different. Because the self-driven force is fixed in the traditional social force model, pedestrians with opposite desired directions are more likely to collide with others, and the simulated average velocity decreases sharply with the increasing of the total number of pedestrians. Due to the intelligent dynamical adjustment of the self-driven force, the modified social force model is capable to reduce unrealistic collisions between pedestrians, and the average velocity is larger than the result by original social force model. For example, the average velocity calculated by our modified model (1.2 m/s) is about twice larger than the result calculated by the original social force model (0.6 m/s). It should be noted that, in a high density situation (e.g., Fig. 13(b), 50 pedestrians in the corridor), a large amount of collisions are generated in bidirectional flow, and the crystallized state or deadlock phenomenon is produced that all pedestrians are nearly blocked by the opposite ones. The average speed will reduce to a small value, which is about 0.1 m/s.

Finally, the fundamental diagram of bidirectional pedestrian flow is calculated to compare our model with the original social force model. During the simulation, the pedestrian flow quantities including density ρ, speed u, flow j were recorded, and the average speed and flow were then calculated. As shown in Fig. 14, an inverse-lambda shape fundamental diagram is observed. It reflects that the maximum flow of $J_{\max} \approx 2$ ped/ms can be obtained, capacity drop occurs near $\rho = 2.4$ ped/m^2 and then the pedestrian traffic turns into the freezing phase. This is similar to the metastable state induced by conflicts among pedestrians. In contrast, using social force model, the maximum flow of $J_{\max}$ is near 1.4 ped/ms, and the critical density is $\rho = 1.2$ ped/m^2. Compared with the original social force model, our model can generate a higher flow and speed. It implies that our model with detour behavior can reduce the conflicts between pedestrians and produce more realistic crowd dynamics.

5. Conclusion

In this paper, a modified social force model is proposed to describe the typical detour behavior in the dynamic characteristics of pedestrian flows. In the model, the space of pedestrian is divided into a series of Voronoi cells, the adjusted desired velocity direction of self-driven force is given by the Voronoi nodes, and the desired velocity is also modified by the consideration of detour behavior. The modification of self-driven force allows the model to predict more reasonable behavior of detouring or avoiding potential collisions with obstacles and other pedestrians.

Using the modified social force model, the detour behaviors can be found, such as collision avoidance in bidirectional pedestrian flow, passing over obstacles and pedestrians. A segment of real-world video is applied to test the performance of the proposed model. Results indicate that our model can be used to describe the more realistic detour behaviors in the pedestrian studies.

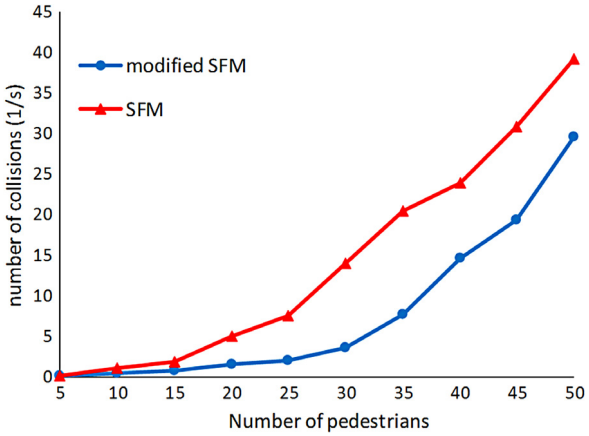

(a) Comparison of the collision times among SFM and modified SFM of bidirectional flow with different number of pedestrians.

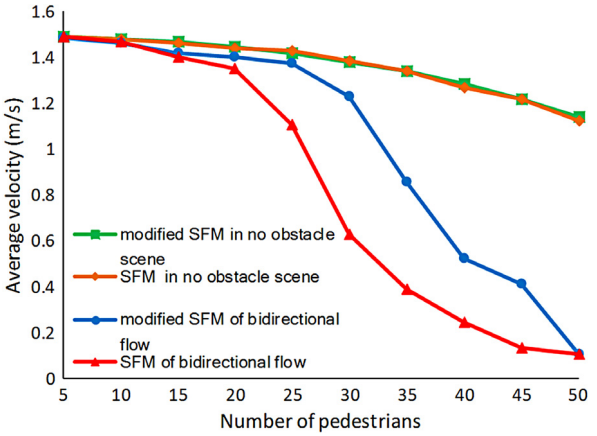

(b) Comparison of the average velocity among SFM of unidirectional flow, modified SFM of unidirectional flow, SFM of bidirectional flow and modified SFM of bidirectional flow.

Fig. 13. Simulation results of bi-directional flow.

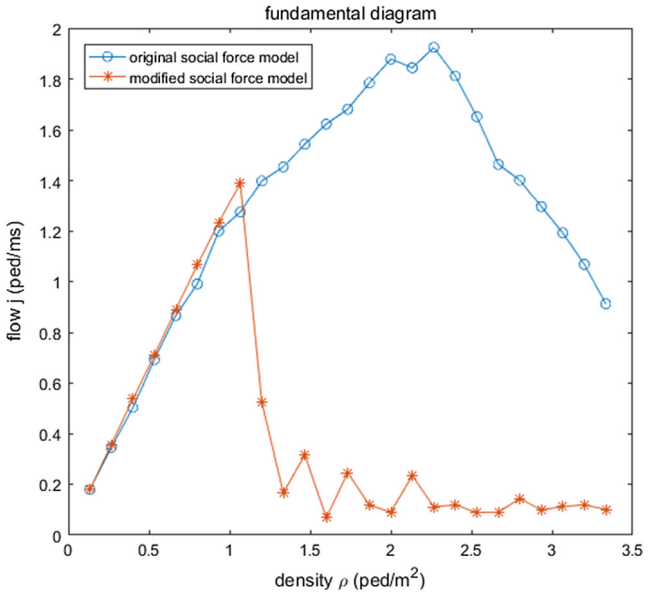

Fig. 14. Fundamental diagram obtained by different models.

This paper discussed the model in three fundamental scenarios, e.g., unidirectional flow in a corridor, bidirectional flow in a corridor, unidirectional flow with static obstacles. In real applications, our model can be used to simulate the scenarios with less bottlenecks, for example, the transfer tunnel in public transit stations. For the homogeneous pedestrian flows, the density of crowd should not be too low or too large. In a low density, pedestrians will move directly to the destination without detouring; while in a high density, pedestrians will form queues to follow others in normal conditions, and detour behavior will be less observed. For the heterogeneous pedestrian flows, the different purposes or motion abilities of pedestrians will increase the occurrence of detour behavior.

The proposed model has good extensibility. Firstly, the heterogeneity and randomness of pedestrian behaviors will be discussed in the future. Other heuristics or rules can be integrated into this Voronoi diagram framework to potentially explore pedestrian dynamics under emergency situations. Besides, this paper only discussed the microscopic motion and detour behavior. Therefore, the microscopic and macroscopic route choice behavior in tactical level, grouping behavior and herding behavior will be another challenging work in the future.

Acknowledgments

This work presented here was made possible thanks to the generous support of the National Natural Foundation Youth Fund (71601017), Science Fund for Creative Research Groups of the National Natural Science Foundation of China (71621001), National Science Foundation for Distinguished Young Scholars (71525002), Chinese Postdoctoral Science Foundation (2017M610042).

References

[1] R.Y. Guo, H.J. Huang, S.C. Wong, Collection, spillback, and dissipation in pedestrian evacuation: A network-based method, Transp. Res. B 45 (2011) 490–506.
[2] A. Johansson, M. Batty, K. Hayashi, B.O. Al, D. Marcozzi, Z.A. Memish, Crowd and environmental management during mass gatherings, Lancet Infect. Dis. 12 (2012) 150.
[3] N. Shiwakoti, R. Tay, P. Stasinopoulos, P.J. Woolley, Likely behaviours of passengers under emergency evacuation in train station, Saf. Sci. 91 (2017) 40–48.
[4] L. Yang, P. Rao, K. Zhu, S. Liu, X. Zhan, Observation study of pedestrian flow on staircases with different dimensions under normal and emergency conditions, Saf. Sci. 50 (2012) 1173–1179.
[5] N. Shiwakoti, M. Sarvi, Enhancing the panic escape of crowd through architectural design, Transp. Res. C 37 (2013) 260–267.
[6] D.C. Duives, W. Daamen, S.P. Hoogendoorn, State-of-the-art crowd motion simulation models, Trans. Res. C 37 (2013) 193–209.
[7] X. Zheng, T. Zhong, M. Liu, Modeling crowd evacuation of a building based on seven methodological approaches, Build. Environ. 44 (2009) 437–445.
[8] H.X. Ge, R.J. Chen, S.M. Lo, A lattice model for bidirectional pedestrian flow on gradient road, Commun. Theor. Phys. 62 (2014) 259–264.
[9] R.Y. Guo, H.J. Huang, Formulation of pedestrian movement in microscopic models with continuous space representation, Transp. Res. C 24 (2012) 50–61.
[10] M. Moussaïd, D. Helbing, G. Theraulaz, How simple rules determine pedestrian behavior and crowd disasters, Proc. Natl. Acad. Sci. USA 108 (2011) 6884.
[11] A. Kirchner, A. Schadschneider, Simulation of evacuation processes using a bionics-inspired cellular automaton model for pedestrian dynamics, Physica A 312 (2002) 260–276.
[12] K. Nishinari, A. Kirchner, A. Namazi, A. Schadschneider, Extended floor field CA model for evacuation dynamics, Ieice Trans. Inf. Syst. D 87 (2003) 726–732.
[13] C. Burstedde, K. Klauck, A. Schadschneider, J. Zittartz, Simulation of pedestrian dynamics using a two-dimensional cellular automaton, Physica A 295 (2001) 507–525.
[14] A. Kirchner, K. Nishinari, A. Schadschneider, Friction effects and clogging in a cellular automaton model for pedestrian dynamics, Phys. Rev. E 67 (2003) 056122.
[15] A. Varas, M.D. Cornejo, D. Mainemer, B. Toledo, J. Rogan, V. Muñoz, J.A. Valdivia, Cellular automaton model for evacuation process with obstacles, Physica A 382 (2007) 631–642.
[16] T. Ezaki, D. Yanagisawa, K. Ohtsuka, K. Nishinari, Simulation of space acquisition process of pedestrians using proxemic floor field model, Physica A 391 (2011) 291–299.
[17] E. Cristiani, B. Piccoli, A. Tosin, Multiscale Modeling of Pedestrian Dynamics, Springer International Publishing, 2014.
[18] W. Li, Y. Li, P. Yu, J. Gong, S. Shen, L. Huang, J. Liang, Modeling, simulation and analysis of the evacuation process on stairs in a multi-floor classroom building of a primary school, Physica A 469 (2016) 157–172.
[19] X. Li, J.Q. Sun, Studies of vehicle lane-changing to avoid pedestrians with cellular automata, Physica A 438 (2015) 251–271.
[20] X. Song, L. Ma, Y. Ma, C. Yang, H. Ji, Selfishness- and selflessness-based models of pedestrian room evacuation, Physica A 447 (2016) 455–466.
[21] T.Q. Tang, L. Chen, R.Y. Guo, H.Y. Shang, An evacuation model accounting for elementary students' individual properties, Physica A 440 (2015) 49–56.
[22] T.Q. Tang, Y.X. Shao, L. Chen, Modeling pedestrian movement at the hall of high-speed railway station during the check-in process, Physica A 467 (2017) 157–166.
[23] K. Zhu, Y. Yang, Q. Shi, Study on evacuation of pedestrians from a room with multi-obstacles considering the effect of aisles, Simul. Model. Pract. Theory 69 (2016) 31–42.
[24] D. Helbing, P. Molnár, Social force model for pedestrian dynamics, Phys. Rev. E 51 (1995) 4282.
[25] D. Helbing, I. Farkas, T. Vicsek, Simulating dynamical features of escape panic, Nature 407 (2000) 487.
[26] D. Helbing, L. Buzna, A. Johansson, T. Werner, Self-organized pedestrian crowd dynamics: Experiments, simulations, and design solutions, Transp. Sci. 39 (2005) 1–24.
[27] T.I. Lakoba, D.J. Kaup, N.M. Finkelstein, Modifications of the Helbing-Molnár-Farkas-Vicsek social force model for pedestrian evolution, Simul. Trans. Soc. Model. Simul. Internat. 81 (2005) 339–352.
[28] L. Hou, J.G. Liu, X. Pan, B.H. Wang, A social force evacuation model with the leadership effect, Physica A 400 (2014) 93–99.
[29] X. Yang, H. Dong, Q. Wang, Y. Chen, X. Hu, Guided crowd dynamics via modified social force model, Physica A 411 (2014) 63–73.
[30] F. Johansson, A. Peterson, A. Tapani, Waiting pedestrians in the social force model, Physica A 419 (2015) 95–107.
[31] Y. Qu, Z. Gao, Y. Xiao, X. Li, Modeling the pedestrian's movement and simulating evacuation dynamics on stairs, Saf. Sci. 70 (2014) 189–201.
[32] M. Li, Y. Zhao, L. He, W. Chen, X. Xu, The parameter calibration and optimization of social force model for the real-life 2013 Ya'an earthquake evacuation in China, Saf. Sci. 79 (2015) 243–253.
[33] W.J. Yu, R. Chen, L.Y. Dong, S.Q. Dai, Centrifugal force model for pedestrian dynamics, Phys. Rev. E 72 (2005) 026112.
[34] M. Chraibi, A. Seyfried, A. Schadschneider, Generalized centrifugal-force model for pedestrian dynamics, Phys. Rev. E 82 (2010) 046111.
[35] J.K.K. Yuen, E.W.M. Lee, The effect of overtaking behavior on unidirectional pedestrian flow, Saf. Sci. 50 (2012) 1704–1714.
[36] Q.L. Wang, Y. Chen, H.R. Dong, M. Zhou, B. Ning, A new collision avoidance model for pedestrian dynamics, Chin. Phys. B 24 (2015) 453–462.
[37] T. Kretz, Pedestrian traffic: on the quickest path, J. Stat. Mech. Theory Expe. 2009 (2009) P03012.
[38] D. Hartmann, J. Mille, A. Pfaffinger, C. Royer, Dynamic medium scale navigation using dynamic floor fields, in: Pedestrian and Evacuation Dynamics, 2012, pp. 1237–1249.
[39] E.L. Mills, G. Rosenberg, A.P. Spidle, M. Ludyanskiy, Y. Pligin, B. May, Simulation of spatial and temporal separation of pedestrian counter flow through a bottleneck, Physica A 415 (2014) 428–439.
[40] W. Guo, X. Wang, X. Zheng, Lane formation in pedestrian counterflows driven by a potential field considering following and avoidance behaviours, Physica A 432 (2015) 87–101.
[41] J.V.D. Berg, S.J. Guy, M. Lin, D. Manocha, Reciprocal n-body collision avoidance, Springer Tracts Adv. Robot. 70 (2015) 3–19.
[42] S.J. Guy, S. Curtis, M.C. Lin, D. Manocha, Least-effort trajectories lead to emergent crowd behaviors, Phys. Rev. E 85 (2012) 016110.

[43] J. Zhang, W. Klingsch, A. Schadschneider, A. Seyfried, Transitions in pedestrian fundamental diagrams of straight corridors and T-junctions, Statistics 2011 (2011) P06004.
[44] J. Liddle, A. Seyfried, B. Steffen, Analysis of Bottleneck Motion using Voronoi Diagrams, Springer, US, 2011.
[45] Y. Xiao, Z. Gao, Y. Qu, X. Li, A pedestrian flow model considering the impact of local density: voronoi diagram based heuristics approach, Transp. Res. C 68 (2016) 566–580.
[46] S.P. Hoogendoorn, P.H.L. Bovy, Pedestrian route-choice and activity scheduling theory and models, Transp. Res. B 38 (2004) 169–190.
[47] A. Okabe, B. Boots, K. Sugihara, S.N. Chiu, Spatial Tessellations: Concepts and Applications of Voronoi Diagrams, John Wiley & Sons, Inc, 2001.
[48] N. Guo, Q.Y. Hao, R. Jiang, M.B. Hu, B. Jia, Uni- and bi-directional pedestrian flow in the view-limited condition: Experiments and modeling, Transp. Res. C 71 (2016) 63–85.